Seasonal Variation in Radiative and Turbulent Exchange at a Deciduous Forest in Central Massachusetts

KATHLEEN E. MOORE, DAVID R. FITZJARRALD, AND RICARDO K. SAKAI

Atmospheric Sciences Research Center, State University of New York at Albany, Albany, New York

MICHAEL L. GOULDEN, J. WILLIAM MUNGER, AND STEVEN C. WOFSY

Division of Applied Sciences, Harvard University, Cambridge, Massachusetts

(Manuscript received 7 February 1995, in final form 17 July 1995)

ABSTRACT

Temperate deciduous forests exhibit dramatic seasonal changes in surface exchange properties following on the seasonal changes in leaf area index. Nearly continuous measurements of turbulent and radiative fluxes above and below the canopy of a red oak forest in central Massachusetts have been ongoing since the summer of 1991. Several seasonal trends are obvious. Global solar albedo and photosynthetically active radiation (PAR) albedo both are good indicators of the spring leaf emergence and autumnal defoliation of the canopy. The solar albedo decreases throughout the summer, a change attributed to decreasing near-infrared reflectance since the PAR reflectance remains the same. Biweekly satellite composite images in visible and near-infrared wavelengths confirm these trends. The thermal emissions from the canopy relative to the net radiation follow a separate trend with a maximum in the midsummer and minima in spring and fall. The thermal response number computed from the change in radiation temperature relative to the net radiation is directly related to the Bowen ratio or energy partition. The subcanopy space follows a different pattern dictated by the presence of the canopy; there the midday sensible heat flux is a maximum in spring and fall when the canopy is leafless, while subcanopy CO_2 flux is maximum in midsummer. Subcanopy evapotranspiration did not have a distinct seasonal peak in spring, summer, or fall. The temperature dependence of the respiration rate estimated from the eddy correlation subcanopy CO_2 flux is comparable to that found using nocturnal flux measurements.

The surface energy balance follows a seasonal pattern in which the ratio of turbulent sensible heat flux to the net radiation (Q_H/Q_*) is a maximum in the spring and fall (0.5–0.6), while the latent heat flux (Q_E) peaks in midsummer ($Q_E/Q_* = 0.5$). This pattern gives rise to a parabolic growing season shape to the Bowen ratio with a minimum in early August. Growing season changes in the canopy resistance (R_c), related to the trends in the Bowen ratio, are more likely to be predicted using the thermal channels of remote sensing instruments than the shorter-wavelength bands.

1. Introduction

Describing and predicting land surface–atmosphere exchange is a critical challenge for understanding global change. The large spatial scales and inherent heterogeneity of the biosphere requires the use of remote sensing to study global change processes. Because remote sensing platforms such as satellites do not measure surface exchange processes directly, research has focused on the parameterization of exchange coefficients, such as the canopy resistance to water vapor transfer (e.g., Verma et al. 1993). The parameterizations are expressed in terms of remotely sensed entities such as reflectance ratios or thermal emission properties.

A desirable feature of observational global change studies is that they must be long term. Very few long-term studies have been conducted of the fluxes of heat, momentum, and trace gases over natural vegetation using direct eddy correlation measurements. Several large-scale studies have been mounted that address the problem of trying to remotely sense biophysical phenomena over selected periods in a single growing season, for example, FIFE (Sellers et al. 1992) and BOREAS (Sellers et al. 1995). The work being reported here makes a contribution to the large-scale studies because of its long-term nature and because we have made simultaneous measurements of the turbulent energy fluxes and the components of the net radiation. Coupling the heat and mass transfer observations to those of radiative exchange provides a bridge to the global-scale observations of natural vegetation by satellite.

Making the connection between remote sensing and biosphere processes also will be useful for studies of

Corresponding author address: Dr. Kathleen E. Moore, Atmospheric Sciences Research Center, SUNY–Albany, 100 Fuller Road, Albany, NY 12205.
E-mail: moore@boojum.asrc.albany.edu

regional-scale variations as the land surface types change, through alteration of evapotranspiration regimes and perhaps the carbon budget. Deciduous forests in the northeastern United States are known to have undergone tremendous changes in the last 100 years, not only in total area but also in species composition (Foster 1992). These forests now occupy more than twice the area that they did 100 years ago. In the case of Harvard Forest in central Massachusetts, a significant rate of carbon uptake is still occurring; that is, the forest is in an aggrading state (Wofsy et al. 1993).

The overriding feature of deciduous forest canopies, and one that can be easily detected via remote sensing, is the seasonally changing leaf area index (LAI), which has a dramatic effect not only on the above-canopy fluxes but also on subcanopy exchange processes through its influence on the radiation environment below and through the restriction of momentum exchange. The subcanopy exchange tells a story about the condition of the canopy above. The subcanopy environment is also interesting in its own right because it possesses the major source for several trace gases, including CO_2 and some oxides of nitrogen. Furthermore it is important to determine the role of the understory and soil surface in the total observed evapotranspiration. (Baldocchi and Meyers 1991). Lastly, subcanopy space comprises a set of unique biological niches that are bounded by the physical changes wrought by the overstory (Fitzjarrald and Moore 1995). Long-term studies of subcanopy exchange have not been done to this point.

Our objective is to document the seasonal changes in energy fluxes at Harvard Forest and to use our measurements as a context for relating the observed fluxes to remote observations, including those from satellites. Specifically, we will illustrate the seasonal variation in turbulent and radiative exchange both above and within the canopy and then show how that variation is detectable from Advanced Very High Resolution Radiometer (AVHRR) biweekly composite data. The paper is complementary to the work of Wofsy et al. (1993) and Munger et al. (1995), who have already reported on the CO_2 uptake and nitrogen chemistry at Harvard Forest.

2. Site and instrumentation

a. Site characteristics

This study is being conducted at the Environmental Monitoring Site at Harvard Forest in Petersham, Massachusetts (42.54°N, 72.18°W), where a 30-m micrometeorological tower has been instrumented since 1990. The immediate forest contains northern red oak (*Quercus rubra*) as its dominant component (80% of the basal area, diameters 45 cm), with an admixture of red maple and hemlock. The forest is 50–70 years old, and average tree height h is 24 m. The LAI is approximately 3.4 (Sakai 1995). The Harvard Forest extends over 1200 ha within the transition hardwood–white pine–hemlock forest region. The nearest paved road is more than 1 km from the tower.

b. Instrumentation

For observations presented in this paper, the group from Harvard University (Goulden, Munger, Wofsy) has maintained instrumentation for flux measurements at 30 m (z/h = 1.25) and the temperature, humidity, and CO_2 gradient measurements on the tower. The group from the State University of New York (SUNY) has operated the radiation sensors above the forest, flux measurement instruments in the canopy and in the soil, and flux data acquisition. An Applied Technologies, Inc. (ATI) three-axis sonic anemometer is located at the tower top from which u, v, w, and T signals are acquired. The temperature signal is that derived from speed-of-sound estimates with the sonic temperature. The instrument is mounted such that the u component is aligned with due west (magnetic). In this orientation the mean wind is within 90° of the positive u component at least 80% of the time. The eddy water vapor signal is from a LiCor 6262 CO_2/H_2O sensor that has an inlet at tower top. The lag time for air to travel down the tube to the sensor inside is about 4 s; covariance estimates for the flux are obtained by lagging the vertical velocity time series with respect to the water vapor series. An ATI three-axis sonic anemometer at the 11-m level is located on the same tower, and a similar instrument is mounted on a 6-m tower 30 m to the west; both of these instruments are oriented due west (magnetic). In addition, during selected periods data from two Campbell Scientific single-axis sonics have been acquired; these were located on the top of 6-m masts 30 m to the north and south of the large tower. During most of 1992 a LiCor 6252 CO_2 sensor with an inlet at the 11-m level on the tower was in operation. For certain periods of time Campbell Scientific krypton hygrometers have been located at the 6-, 11-, and 30-m levels to provide additional measurements of the water vapor flux.

A boom supporting several radiometers is attached to the large tower at 27 m. This suite of instruments consists of upward- and downward-looking Kipp and Zonen pyranometers (model CM-11), Eppley model PIR pyrgeometers, and LiCor model LI190SA quantum PAR (400–700 nm) sensors. A Swissteco net radiometer has also been deployed on this boom for long periods. The radiation data and soil temperature and heat flux data are acquired by Campbell Scientific data loggers with a 20-min-averaging period. Table 1 lists the instruments and their locations on the towers.

The SUNY group has collected data continuously since July 1991 for radiation measurements and 2 August 1991 for turbulence measurements, with periods of lost data due to lightning damage, power failure, or

TABLE 1. Instruments and their locations at Harvard Forest.

Large tower
30 m: u', v', w', Tv', T', q', CO_2' (Harvard instruments)
Rn, *S*(up), *S*(down), *L*(up), *L*(down), PAR(up), PAR(down)
11.3 m: u', v', w', Tv', T', q', CO_2'
Auxiliary tower (30 m west of large tower)
6.6 m: u', v', w', Tv', T', q', CO_2'
Auxiliary mast (30 m north of large tower)
3 m: w', T'
Auxiliary mast (30 m south of large tower)
3 m: w', T'
Soil measurements
3 temperatures (2- and 8-cm depth), soil heat flux (5-cm depth)

instrument malfunction. Overall, there has been a data capture rate of 95% for the radiation instruments, 75% for the sonic anemometer at the top, and 50%–70% for other turbulence measurements, depending on the month of the year.

c. Data acquisition and analysis

Turbulence data were acquired at 10 Hz by a PDP11/73 computer, after filtering through a hardware filter with a 5-Hz cutoff. The data stream was sent serially to a Sun IPC workstation where the data were written into a raw data file. A separate program reads the raw data, constructs 1-s average time series, and calculates moments (up to the fourth), spectra, co- and quad-spectra, and flux covariances. In addition, this analysis program performs a coordinate rotation in the manner described by McMillen (1986) to correct the fluxes for nonalignment of the sensor with the flow. Raw data, 1-s averages, and derived data (moments, spectra, fluxes, etc.) are backed up on digital audio tape once a day. Campbell Scientific data logger data are recorded on audio cassette tape. Routine visits to the site are scheduled approximately every 2 weeks to change tapes and perform maintenance. A modem is attached to the workstation so that data quality can be remotely checked several times a week. Programs to graphically display raw time series, spectra, moments and fluxes are run remotely so that plots of these can be examined. Small quantities of data and plots can be retrieved via modem for further examination in Albany. Rotation corrections are 4%–10% for heat and 10%–12% for momentum during the day. The momentum correction results in a change of sign only for certain nighttime cases. The wind direction dependence of the corrections indicates that the top sonic is about 2° out of alignment with the mean flow.

An indication of the quality of the turbulence data for the above-canopy layer can be gained by examining the extent to which the data conform to certain surface-layer similarity relationships. For the small values of $-z/L$ characteristic of midday at Harvard Forest, we find $\sigma_w/u_* = 1.2$, close to the neutral ($-z/L$) prediction of the surface-layer similary hypothesis of 1.3 (Panofsky and Dutton 1984, 161). This is true for most wind directions except those for which the wind is coming from behind the instrument and the tower may interfere (Table 2).

d. Auxiliary datasets

Daily data from many climate stations, including maximum and minimum temperatures, precipitation, and snowfall data for the period 1948 through the end of 1992 were obtained (Earth Info, Inc.). There are six stations within 24 km of Harvard Forest that provide a database for understanding interannual variability, as well as rain and snowfall data for individual days in 1991 and 1992.

Biweekly composite NOAA AVHRR data for the conterminous United States were obtained from the U.S. Geological Survey National Mapping Division EROS data center. These data include normalized difference vegetation index (NDVI), as well as separate outputs for each of the five AVHRR channels with a spatial resolution of 1.1 km. Gallo's (1992) experimental calibrated global vegetation index (GVI) was examined for the period 1985–91. These biweekly satellite composites have a coarser spatial resolution than the EROS dataset, about 15-km pixels in the region of Harvard Forest.

3. Radiation

a. Summer albedo changes

Mean daily midday (1000–1400 LST) global albedo for the period July 1991–December 1993 is shown in Fig. 1. The periods of canopy leaf-out and leaf-drop are easily detected as a rise or fall of albedo, respectively. During the summer, a decrease in albedo of about 11% over the season occurs. The slopes of the least squares fits for the three summers are not significantly different from one another, all being about -0.0002 day^{-1}. The decrease in albedo, while representing a small part of the radiation balance, may signal a change in the physiological state of the canopy.

Most vegetation canopies exhibit bidirectional, as well as specular, reflectance, which is dependent on wavelength; this fact presents a problem for satellite

TABLE 2. Midday σ/u_* by wind direction for the month of August 1991. The sonic is pointed due west (magnetic).

Ratio	1.18	1.43	1.45	1.19	1.17	1.19	1.19	1.21
Wind direction	0°–45°	45°–90°	90°–135°	135°–180°	180°–225°	225°–270°	270°–315°	315°–360°

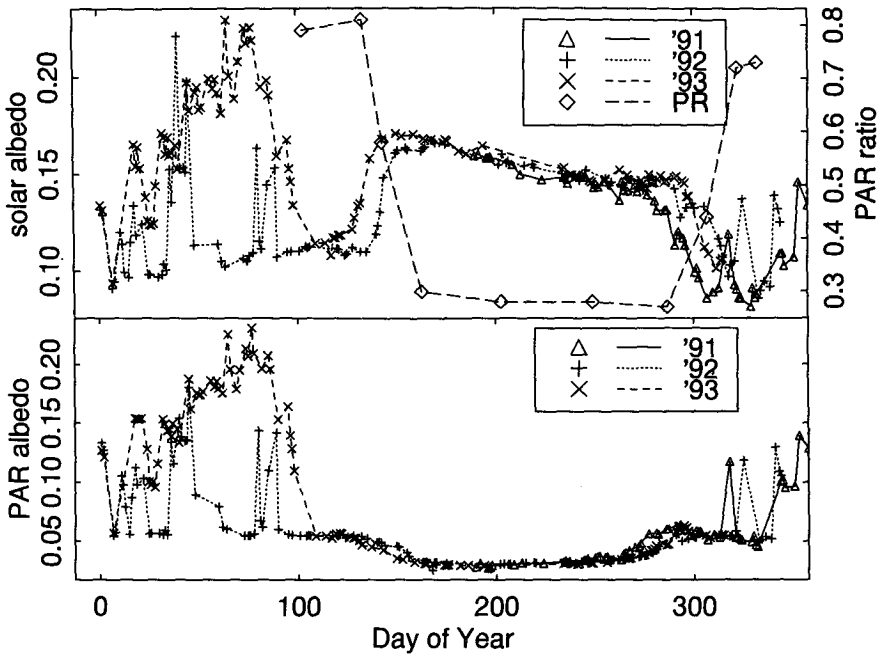

FIG. 1. (Top) Mean daily midday global solar albedo from pyranometers for July 1991–December 1993. Also shown is the ratio of PAR received at 11 m to that above the canopy. (Bottom) PAR albedo for the same period.

and other sensors that have a narrow view angle. We considered the possibility that summer albedo changes depended on solar zenith angle; several lines of evidence suggest that the observed summer global albedo trend is not due to changes in the solar zenith angle. The same trend is observed for both cloudy and sunny days, alleviating the concern that specular reflection is the cause of observed albedo changes. Further, when albedo for 40 clear days in the summer of 1992 is plotted by solar zenith angle (Fig. 2), it is apparent that the trend due to daily solar zenith angle changes is positive, opposite to that over the season. At the high solar zenith angles of the morning, albedo is higher than it is by noon, but albedo remains relatively unchanged during the afternoon hours. The higher morning albedo could be caused by dew. It is not caused by reflectance from the tower since the leafless canopy displays a *minimum* albedo in morning and late afternoon. Another possibility is that there is an azimuthal dependence to the reflectances (consistent with the effect of bidirectional reflectance), perhaps caused by an azimuthal dependence of leaf orientations.

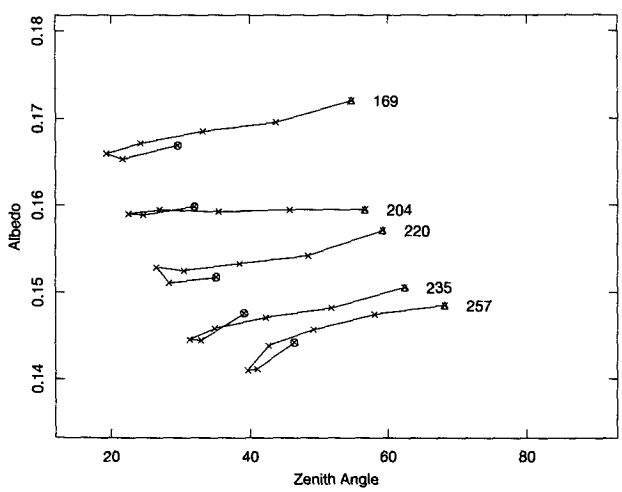

FIG. 2. Hourly albedos (1100–1700 LST) by day of year for five selected sunny days spaced through the summer of 1992 against the solar zenith angle. Each line is labeled by the day of the year. Circles mark 1100 LST, and triangles mark 1700 LST.

Plant reflectivities typically have a sharp transition around 700 nm from low to high [0.35 or greater; Gates (1980)], and data obtained by Waring et al. (1995, personal communication) from an ultralight aircraft over Harvard Forest confirm that the red oak canopy has such a typical reflectance spectrum. Most organic materials absorb in the ultraviolet (UV), some in the visible, and very little in the near-infrared. Neither our measured PAR (400–700 nm) albedo nor the AVHRR channel-1 reflectivity data (580–680 nm) change during the growing season. Channel-2 (700–1100 nm) reflectivity does decrease steeply during summer, confirming that changes in the near-infrared (NIR) reflectance are the cause of the observed albedo change. An average of channels 1 and 2 weighted by the fraction

of the solar spectrum in those bands yields an albedo trend of -0.0004 (standard error 0.0001) day^{-1}, slightly steeper than that observed by our pyranometers (Fig. 3).

There are several possible real contributors to the summer albedo trend observed at Harvard Forest. The first is that the water content of deciduous leaves decreases during the growing season, both because of water stress that can occur with a dropping water table and because the dry matter content of the leaves increases, so that leaves do not have to have a net loss of water to experience a declining water content. Hunt and Rock (1989) showed that near-infrared reflectance could be used to predict water content of leaves of many species; however, they concluded that the water content change required for detection was too great to be applicable in the field. The second possibility is that changes in leaf anatomy, especially in the thickness of the mesophyll layer, may result in increasing absorption of radiation and decreasing reflectance. Oak leaves are known to accumulate lignin in the epidermis as they age, accounting for their leathery texture by autumn (Esau 1965). Third, there may be seasonal changes in canopy structure—leaf-angle distribution (due perhaps to change in leaf turgor), total number of foliage elements, or understory canopy development.

Published reports of similar continuous measurements of forest albedo are rare. McCaughey (1987) reported on an albedo study at a mixed forest in Ontario but did not indicate a growing-season trend in the measurement. Seasonal variation in albedo over a dry tropical deciduous forest was reported on by Barradas and Adem (1992). In this case, the light-colored trunks of the trees caused the leafless albedo to be higher than that for the leafed state, illustrating that the trends we see are dependent on species composition. Single-leaf spectral reflectances for white oak (*Quercus alba*) do not decrease through the growing season once the leaves are fully expanded (Gates 1980), yet the simple biosphere (SiB) model (Dorman and Sellers 1989) computes, based on a two-stream approximation, a declining albedo in "broadleaf deciduous (*Quercus alba*)" forests during the growing season due to loss of canopy elements through senescence and death. This source for a summer albedo decline would be detectable in the visible bands, however, but is not observed at Harvard Forest. It is possible that canopy changes, rather than single-leaf changes, are responsible for the trend observed here, for instance, a low-level endemic population of gypsy moth, but this has not been observed. Further, PAR sensors above and below the canopy were operated during 1992, and the ratio of these measurements follows the above-canopy PAR albedo: decreasing in the spring, remaining constant during the summer, and increasing as the leaves fall off (Fig. 1). These data give no indication that the canopy was opening up during the growing season. Furthermore, Sakai (1995) has analyzed LAI measurements from digital images at Harvard Forest and has found that LAI increases from 2.8 to 3.3 from June to August.

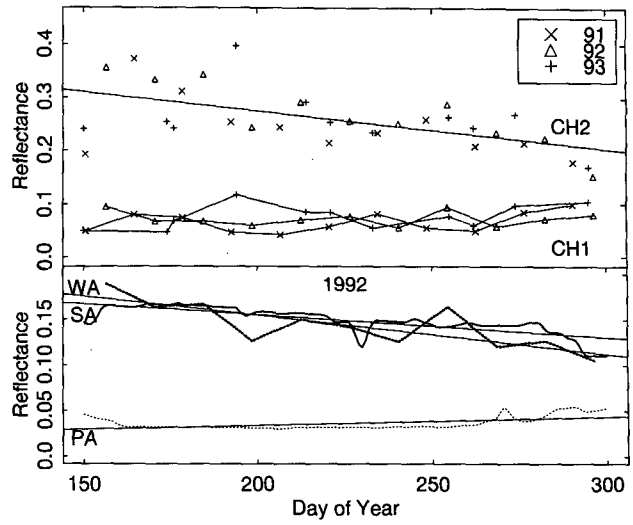

FIG. 3. Growing season reflectances in 1991, 1992, and 1993. (Top) Satellite reflectances from AVHRR channels 1 ("CH1," 580–680 nm) and 2 ("CH2," 725–1100 nm). The regression line for pooled channel-1 reflectances is shown. The equation is reflectance = 0.418 − 0.0007(day of year). (Bottom) SA (heavy solid line) is the pyranometer-based albedo; WA (heavy dashed line) is the weighted average of the NIR and VIS satellite reflectances; PA (dotted line) is the albedo from the PAR instruments. The regression lines for solar and PAR albedos are shown as thin straight lines.

Various measures of the NDVI also decreased during the growing season (days 150–290). The NDVI derived from satellite AVHRR reflectivities, when growing season data for 1991–93 were pooled, showed a significant negative slope of -0.0009 day^{-1}, as did the experimental calibrated global vegetation index of Gallo (1992) (slope -0.0014 day^{-1}) for the composited period 1986–90. The NDVI is an index of greenness constructed from the reflectances in bands 1 (VIS, 580–680 nm) and 2 (NIR, 700–1100 nm) of the AVHRR instrument:

$$\mathrm{NDVI} = \frac{\mathrm{NIR} - \mathrm{VIS}}{\mathrm{NIR} + \mathrm{VIS}}.$$

A similarly scaled vegetation index was constructed using the global solar and the PAR in situ measurements. As expected, this index also decreased with time during the growing season, with a slope of -0.0010 day^{-1}.

b. Summer thermal response changes

The thermal response of the surface skin temperature to net radiative input is indicated by a thermal response number (TRN):

$$\mathrm{TRN} = \frac{(\Sigma Q_* \Delta t)}{\Delta T_0}, \qquad (1)$$

where $\Sigma Q_* \Delta t$ is the total amount of net radiation received during a period of time and ΔT_0 is the change in surface temperature (largely canopy) occurring during that period. The T_0 for Harvard Forest was determined from the downward-looking longwave radiometer, assuming an emissivity of 1.0. Physically, the TRN can be thought of as a kind of surface heat capacity (J K^{-1} m^{-2}); it was first introduced (Luvall and Holbo 1991) as a means of determining the energy partition over vegetation through remote sensing. Consideration of the leaf energy balance (Oke 1987) suggests that with increasing transpiration, leaf surface temperatures should remain cooler relative to the input of net radiation (higher TRN):

$$-Q_* \approx Q_E + Q_H \approx (1 + \beta^{-1})Q_H \approx (1 + \beta^{-1})\frac{(T_L - T_a)}{r_a}, \quad (2)$$

where T_L is leaf temperature, T_a is air temperature, r_a is the aerodynamic resistance (u_*^2/U), Q_* is net radiation, Q_H is the sensible heat flux, Q_E is the latent heat flux, and β is the Bowen ratio (Q_H/Q_E). The approximation refers both to the fact that we have substituted the canopy radiation temperature for the bulk canopy heat exchange temperature typically employed in the Penman–Monteith equation and to the fact that storage Q_G is ignored in (2). Integrating through time and assuming that T_a stays constant over the period of integration, we have

$$-\int Q_* dt \approx \frac{(1 + \overline{\beta^{-1}})}{r_a} \Delta T_L,$$

then

$$\text{TRN} \approx \frac{(1 + \beta^{-1})}{r_a} \approx \left[r_a \left(\frac{Q_H}{-Q_*} \right) \right]^{-1}.$$

During the 1992 and 1993 growing seasons, the TRN increased early in the growing season, as leaves expanded and more energy was partitioned into transpiration, then decreased after late July, as leaves became lignified and probably drier (Fig. 4). This interpretation is supported by data on the seasonal pattern of Q_H/Q_* or a fraction of net radiation partitioned into sensible heat, also shown in Fig. 4. The peak in TRN may be the first indication of the onset of leaf senescence, as leaves begin to become less efficient at water vapor transfer at this time. This is discussed further below.

c. *Winter snow albedo*

Studies of the ripening snow pack are important because an absorption–temperature feedback exists such that snow ripens more quickly as albedo decreases and more radiation is absorbed (Kuhn 1989). This process contributes to highly spatially and temporally variable albedos that must be accounted for in global climate models. In this study, snowfall events were identified for six stations in central Massachusetts within 24 km of the Harvard Forest (NCDC Summary of the Day, EarthInfo, Inc.). After leaf-fall, large changes in the solar albedo are observed due to periodic snowfall events (Fig. 1). The total albedo never goes higher than about 0.25, even after snow, as the dark branches of the trees contribute substantially to the surface albedo. Without snow and without leaves the surface albedo goes as low as 0.05. The albedo following snow events declines, in part because the snow falls off the dark branches and in part because as the snow surface ages it collects aerosols. Furthermore, the surface of the snow can melt in sunlight, resulting in a lowered reflectivity. The time constant for this decline is on the order of 2–3 days. The variation in time constant is unrelated to the depth of the snowfall or the water content of the snow (determined from the total precipitation data from the six stations). These results are similar to those reported by McCaughey (1987) for a mixed forest in Ontario. He reported that the albedo decreased to its minimum value within 4 days. The average rate of decline is much greater than that reported for deciduous forest by Robinson and Kukla (1984) following a single snowfall in February of 1983. Although satellite visible reflectivities (AVHRR channel 1) change with the presence or absence of snow, our in situ measurements provide a much finer time resolution than can be achieved with the biweekly composites.

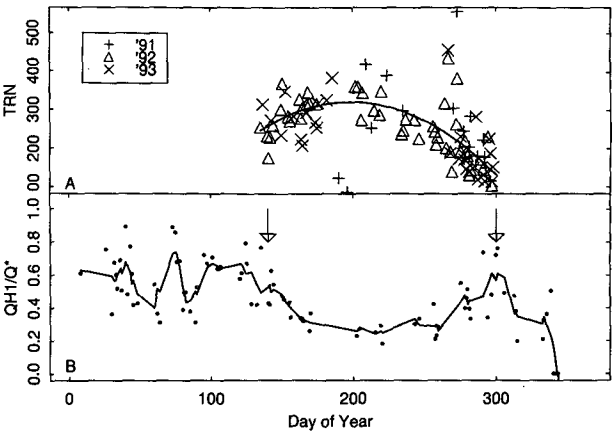

FIG. 4. (a) Growing-season thermal response numbers TRN (J K^{-1} m^{-2}) for 1991, 1992, and 1993. Line is the best-fit quadratic for the 1992 data: TRN = −410.9 + 7.389(day) − 0.0186(day^2), multiple R^2 = 0.45. (b) Sensible heat flux at 30 m as a fraction of net radiation during 1992. The line represents smoothed data. The arrows depict the approximate dates of leaf emergence and leaf drop.

4. Turbulent exchange

a. *Heat budget at canopy top*

The heat budget at the top of the canopy can be written (Oke 1987)

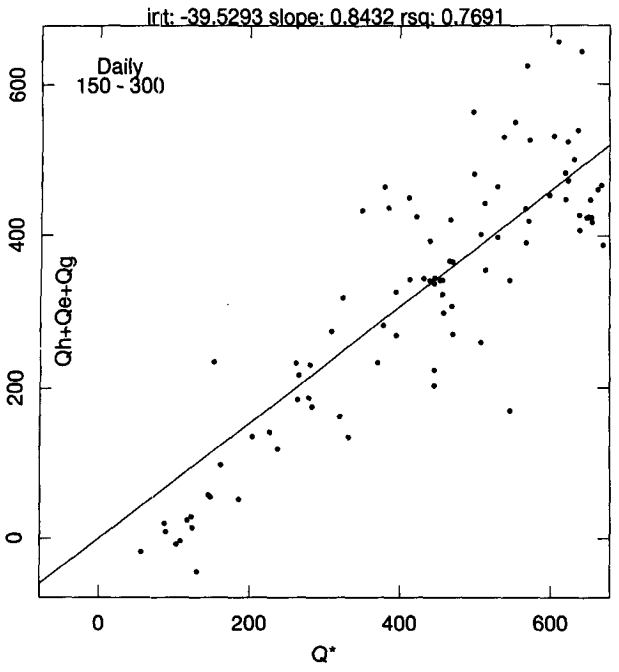

FIG. 5. Heat budget statistics for the growing season of 1992. Daily midday (1000–1400 LST) mean Q_* and the sum of turbulent sensible and latent heat and soil heat flux (5-cm depth) are presented.

$$Q_* = Q_H + Q_E + Q_G + Q_S,$$

which simply states that the net radiation received at a given level is balanced by the turbulent fluxes of sensible heat and latent heat, as well as the storage in the ground and in the biomass (Q_S). In general it is thought that the first three terms on the right-hand side of this balance account for more than 95% of the net radiation.

Measured heat budgets over forest frequently are not balanced for a variety of reasons (Fitzjarrald and Moore 1994; Laubach et al. 1994), and the site at Harvard Forest is no exception. Individual days do exhibit fairly balanced heat budgets (residual of 10% of net radiation or less), but other days do not. A stability-dependent empirical correction scheme (Moore 1986) was applied to the 1992 growing season data; the closure approaches 84% for midday means (Fig. 5). This scheme was developed from transfer functions to overcome problems in frequency response, path averaging, and sensor spatial separation. The budget residuals as a fraction of the net radiation are greatest when the wind is from the southwest. An investigation into the effect of surface-type variation on the budget residuals is underway. Certain periods exhibit better closure than others; for example, the mean daily sum of the turbulent and soil heat fluxes accounts for 93% of the net radiation in autumn days 250–300 (while leaves are still on the trees) in 1992. As Fitzjarrald and Moore (1994) pointed out in their time series of budget residuals in a boreal lichen woodland, significant storage or advection can result in the budget being out of balance for long periods.

There are several possible reasons for the imbalance, including significant differences between the footprint for the net radiation measurements compared to that for the flux and significant storage of heat in the biomass (this could account for up to 10% of the residual). The net radiometer receives 95% of its signal from a canopy-top area of about 100 m (Latimer 1978), centered at the tower, while the turbulent flux measurements probably apply to an area at least twice as large, or more, at midday, centered upwind of the tower. These discrepancies are still under review, but their existence does not alter the conclusions of this paper.

A seasonal heat budget for sunny days in 1992 is shown in Fig. 6. Sunny days are defined as those days for which the midday global solar radiation is 70% or more of the top of atmosphere value for that day. Though measurements are made continuously, in this figure sunny days are shown to take out some of the variability and highlight the outer limits of net radiation and heat flux during the year. The Bowen ratio (Q_H/Q_E) is also shown in Fig. 6. Evidently transpiration picks up slowly, requiring fully expanded and developed leaves. For a period of 2 weeks in late spring and early summer, energy partition into latent heat flux increases. Transpiration then begins to decline in the month of August as leaves become more lignified. The decrease in latent heat flux corresponds to a period of decreasing TRN, as mentioned above. Direct measurements of latent heat flux support these conclusions (Fig. 7). The data in Fig. 7 suggest that the slope between TRN and Q_E in the late summer and autumn

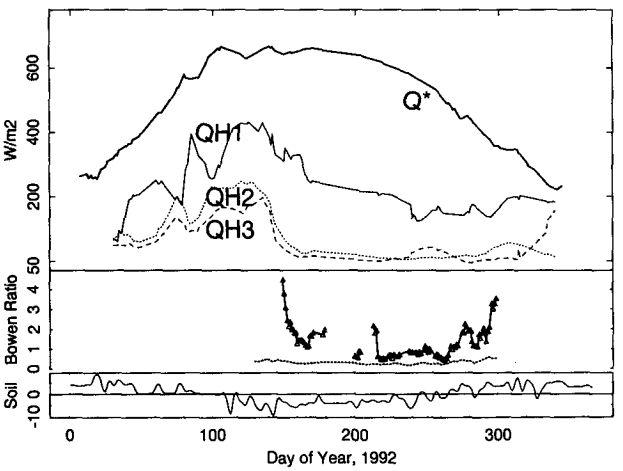

FIG. 6. Seasonal heat budget for sunny days at Harvard Forest in 1992. Term Q^* is the net radiation, QH1 is the sensible heat flux at 30 m, QH2 is for 11 m, and QH3 is from a 6-m auxiliary tower. The middle graph shows the measured Bowen ratio during the growing season (solid line) and the "equilibrium" Bowen ratio (dashed line). The soil heat flux (W m^{-2}) at 5-cm depth is shown at the bottom.

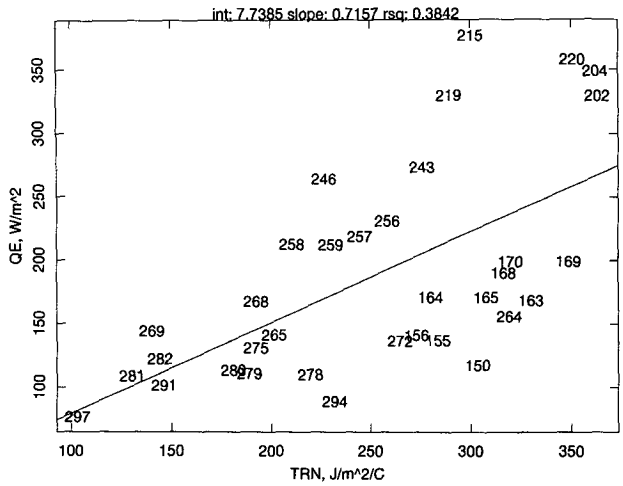

FIG. 7. Thermal response number TRN (J K^{-1} m^{-2}) versus latent heat flux at 30 m for sunny days in the growing season of 1992. The straight line is the least squares regression for the data. Numbers identify the day of year.

(days after 240) may be different than it is in spring and early summer (days before 200).

The drag coefficient, $C_D = u_*^2/U^2$, where u_* is the friction velocity and U is the mean horizontal wind speed, is a measure of the efficiency of exchange between the atmosphere and the surface. Despite the dramatic changes associated with the development of a full canopy, the daytime drag coefficient above the canopy does not change with the presence of canopy (Fig. 8), a result consistent with that of Shaw et al. (1988) obtained at a deciduous forest in Ontario. The displacement height, determined from wind profiles in neutral conditions, does change, from about 14 m just before leaf-out to 19.8 m fully leafed. This indicates that although momentum penetrates deeper into the forest in winter than in summer the forest is no more effective at removing momentum from the atmosphere then. Wind direction does have a significant effect on the measured drag coefficient, probably a result of instrument interference. Data from the easterly wind directions have been eliminated from the analyses.

Lu and Fitzjarrald (1994) found that vertical and horizontal motions within the canopy at Harvard Forest provoked by coherent structures are twice as large in winter compared to summer. The ratio of the mean wind speed below and above the canopy ranges from 0.5 to 0.15 as the leaves come out. As with the heat flux ratio (Q_H at 11 m divided by Q_H at 30 m, discussed below), there was a period of 1–2 weeks in spring of 1992 before leaf emergence when the ratio increased from 0.3 to 0.5. During this period subcanopy convective activity was enhanced as the solar elevation angle and direct heating of the ground increased.

b. *Evapotranspiration*

Growing-season Bowen ratio for 1992 is shown in Fig. 6. The minimum Bowen ratio was reached in early August. Total evapotranspiration (ET) for days 150–300 in 1992 was 244 mm, a figure obtained by applying the mean daily ET for the 12 days of missing water vapor flux data for that period. The mean precipitation from six nearby climate stations was 502 mm, indicating that evapotranspiration was slightly less than 50% of precipitation during this period. Long-term records of direct ET measurements are not available for this ecosystem; however, long records (1956–94) of precipitation and streamflow for eight gauged watersheds in New Hampshire are available from the Hubbard Brook Experimental Forest, approximately 150 km north of Harvard Forest. The ET can be approximated as the difference between precipitation and streamflow (Bormann and Likens 1979). The Hubbard Brook records indicate that since streamflow is very low in the summer, ET is close to 100% of precipitation for the months of June–October, amounting to an average total growing season ET around 400 mm.

The Penman–Monteith equation (Peixoto and Oort 1992) for evaporation allows us to examine the apparent difference in ET at Harvard Forest as compared to Hubbard Brook:

$$Q_E = \frac{\Delta}{(\gamma + \Delta)} A + \frac{\gamma}{(\gamma + \Delta)} \rho L_V \frac{(q_s - q_a)}{R_c}, \quad (3)$$

where Δ is the change of saturation vapor pressure with temperature ($=de_s/dT$) from the Clausius–Clapeyron equation; γ is the psychrometric constant; A is the available energy ($=Q_* - Q_G$); L_V is the latent heat of evaporation; q_s and q_a are the saturation and atmospheric specific humidities, respectively; and R_c is the

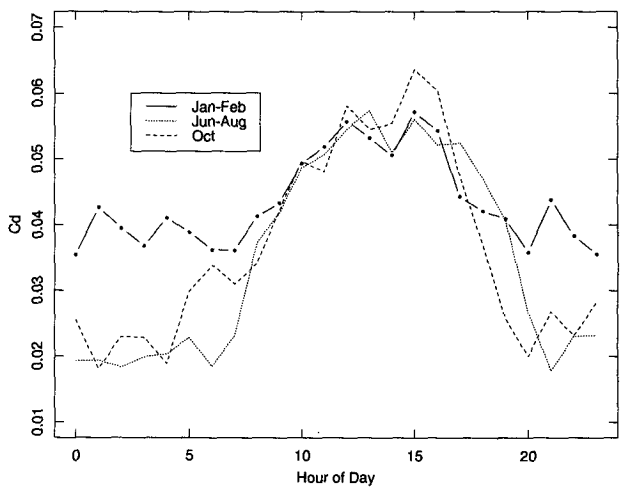

FIG. 8. Drag coefficient by hour of day during 1992. Values represent the median for the selected period.

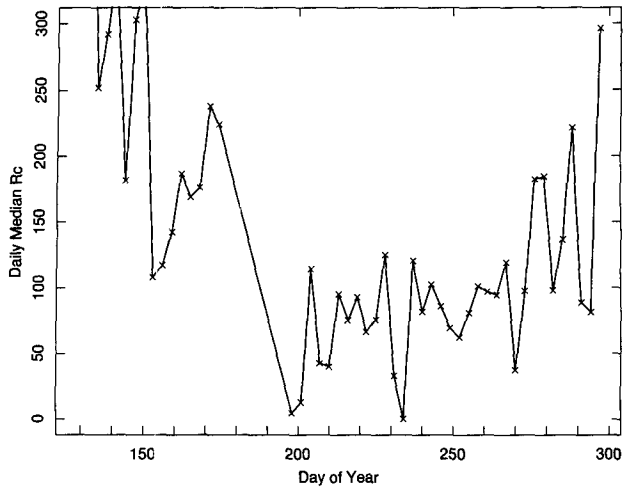

FIG. 9. Canopy resistance to water vapor transfer (s m^{-1}) during the growing season of 1992. Three-day median midday values are shown.

canopy resistance to water vapor transfer. When the equation is written in this way, one can refer to the first term as the "equilibrium term" and the second as the "aerodynamic term," which indicates the "drying power" of the atmosphere (Peixoto and Oort 1992). The term $(\Delta/\Delta + \gamma) \equiv \epsilon$ is determined solely by the temperature of the air; it gives the evaporative fraction Q_E/Q_*, which would be expected over a freely evaporating wet surface, what has been termed "equilibrium evaporation." The value $1/\epsilon$, the Bowen ratio expected under those conditions, is shown as a dashed line in Fig. 6. The graph indicates that evaporation is closest to equilibrium during early August but that the Bowen ratio is significantly greater than the equilibrium value in early and late summer. In order for the Harvard Forest ET to reach the high fraction of total precipitation apparently achieved by the Hubbard Brook ecosystems, evapotranspiration would have to be equilibrium for the entire growing season.

The apparent difference in ET measured by direct means at Harvard Forest and that obtained indirectly from Hubbard Brook ecosystems is intriguing and deserves further study. If the LAI at Hubbard Brook were larger than that at Harvard Forest, then ET would be expected to be a higher fraction of net radiation there. Our ET measurement could be an underestimate, but only by a few percent since Q_E is constrained by the heat budget. Surface and subsurface runoff probably account for some of the difference between precipitation and evapotranspiration at Harvard Forest. This is an area that demands further work if ET is to be scaled up to the regional scale.

The Priestley–Taylor formulation for (3) is $Q_E = \alpha(\Delta/\Delta + \gamma)(Q_* - Q_G)$, in which the parameter α is introduced to indicate the extent to which evaporation is greater or less than equilibrium. When data from only *sunny* days between days 200 and 297 were put together, the value for α is 1.27 (comparable to other studies), indicating a significant "drying power" of the atmosphere. This tendency of α to be greater than one can be attributed to entrainment of dry air at the top of the boundary layer (e.g., DeBruin 1983) and has been the subject of several model studies (Culf 1994; Betts 1994). Further work on understanding the approach to equilibrium over several-day synoptic sequences at Harvard Forest is in progress.

A rearrangement of (3) provides a means to estimate the bulk canopy resistance to water vapor transfer when the latent heat flux is known (Monteith 1965). The goal of much of the research on remote sensing of biophysical processes in vegetation has been to find parameterizations for, or surrogate measures of, R_c:

$$R_c = \rho c_p \frac{\Delta}{(\gamma Q_E)} + R_{aM}\left[\left(\frac{\beta}{\gamma}\right)\left(\frac{de_s}{dT}\right) - 1\right], \quad (4)$$

where ρc_p is the volumetric heat capacity of air, Δ is the saturation deficit, γ is the psychrometric constant, R_{aM} is the aerodynamic resistance $(=U/u_*^2)$, β is the Bowen ratio, de_s/dT $(\equiv s)$ is given by the Clausius–Clapeyron equation. The midday mean R_c for the 1992 growing season is shown in Fig. 9.

Over forests, with their relatively low aerodynamic resistances (R_{aM} is less than 10 s m^{-1} here), the first term in (4) above is the most important. The latent heat flux increases, while the sensitivity to saturation deficit decreases to the early August point. After this time, R_c and its sensitivity to Δ increases again, with the increasing Bowen ratio, declining Q_E, and increasing TRN. The parabolic growing season trends are observed in these variables, but a different trend is observed in Q_*, albedo, and NIR reflectance; the latter

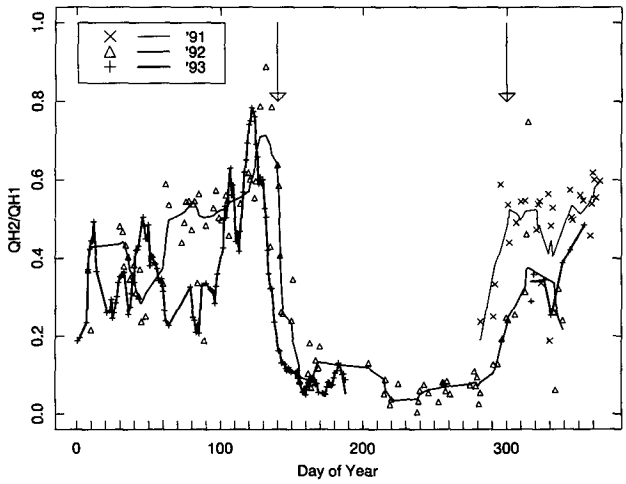

FIG. 10. Ratio of sensible heat flux at 11 m (QH2) to that at 30 m (QH1) for the period August 1991–December 1993. Arrows denote time of leaf emergence and leaf drop in 1992.

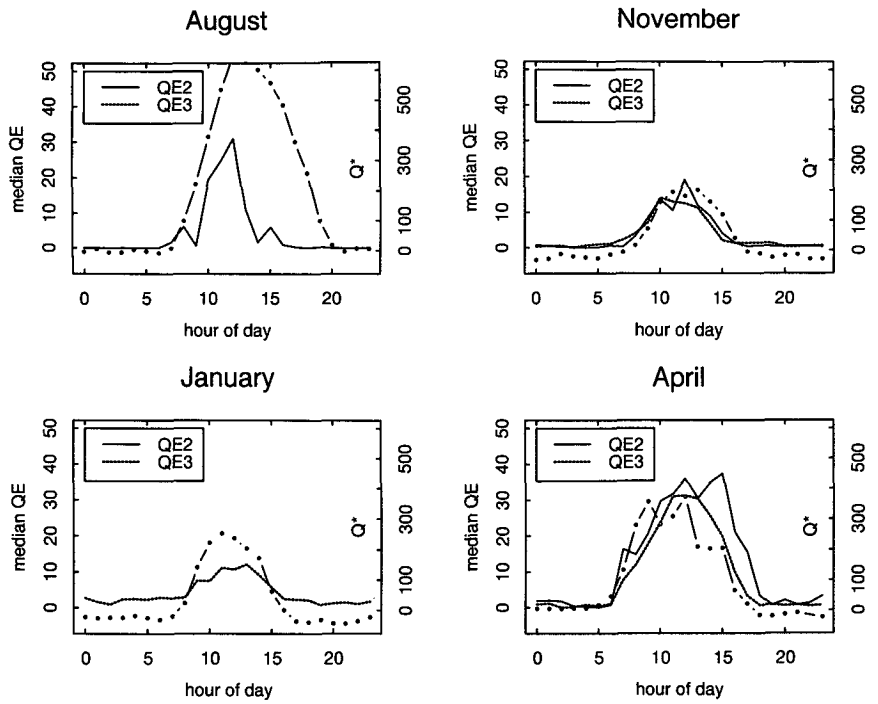

FIG. 11. Hourly median subcanopy latent heat flux (W m^{-2}) for selected months in late 1991 and early 1992. The net radiation at 30 m (W m^{-2}) is shown with the dash–dot line. QE2 is the estimate from 11 m; QE3 is from a 6-m auxiliary tower.

variables have a monotonic linear decline with time during the growing season. As a result, the seasonal relationships among the water-related variables (Q_E, TRN, Tbb, R_c) are more significant than those with the shorter-wavelength reflectances. Changes in canopy resistance in relation to LAI changes during the transition seasons are discussed by Sakai (1995).

The thermal infrared channels of the satellite AVHRR instrument can be used to determine surface temperature, which is in part a function of the energy partition (Bowen ratio), through the leaf surface energy balance. Nemani and Running (1989) have used the slope of the NDVI versus surface temperature across an area at a given time to predict the canopy resistance under different soil moisture conditions. Since the thermal response number is directly correlated with the observed latent heat flux (Fig. 7), this remotely sensed variable could be a surrogate measure of evapotranspiration.

A potentially simpler surrogate for the latent heat flux is the longwave temperature of the canopy derived from the downward-looking pyrgeometer. We find good agreement between the satellite thermal IR temperatures for the Harvard Forest pixel and our longwave temperatures. The Eppley longwave temperature predicts the latent heat flux ($R^2 = 0.61$, $p < 0.01$), although with more scatter in the data than is seen if TRN is used as the predictor.

c. *Seasonal variation in subcanopy exchange*

The emergence of leaves in the spring has a dramatic effect on the subcanopy environment, as solar radiation is blocked and momentum is absorbed near canopy top. In the weeks prior to leaf emergence, as solar elevation angle increases, the subcanopy heat flux approaches 70% of that above the forest (Fig. 10). Within a week as leaves emerge, the ratio of the two heat fluxes decreases to 10% and remains low throughout the summer until leaf drop, when the ratio increases again. The rapid drop of subcanopy heat flux following leaf emergence contrasts with the slower decrease in Bowen ratio at canopy top; the overstory appears to function fully as a shade canopy before it becomes most effective as a source of water vapor.

When the canopy is leafless, most of the total evaporation is due to evaporation from the soil surface. During the winter of 1991/92 we operated krypton hygrometers at the 6-m level on the auxiliary tower and at the 11-m level on the main tower, alongside our three-axis sonic anemometers. Problems with the instruments limited the amount of time that both of them were operating simultaneously. Nonetheless, between the two sets of instruments most of the winter had subcanopy evaporation measurements. Some of the results are shown in Fig. 11. Median midday values of the latent heat flux at the two locations were within 5

W m^{-2} of one another, a result that increases our confidence in the representativity of the subcanopy flux measurements, at least when the overstory is leafless. The evaporation was 3%–10% of the net radiation at the top of the canopy, and subcanopy Bowen ratios were greater than three during the day (e.g., in February 1992). By midsummer, subcanopy Q_E was 40–50 W m^{-2}, so that subcanopy evapotranspiration accounted for only 10%–11% of the above-canopy water vapor flux over the growing season.

Subcanopy sensible heat flux is a maximum at the spring and fall transitions, when the canopy is leafless, because of the higher solar elevation angles; the subcanopy CO_2 flux has the inverse seasonal pattern, however, being a maximum in the midsummer when there is the most biological activity in the subcanopy layer. Subcanopy Q_E does not have a distinct midsummer or spring and fall peak. Lower Q_E in winter is probably due to frozen soil.

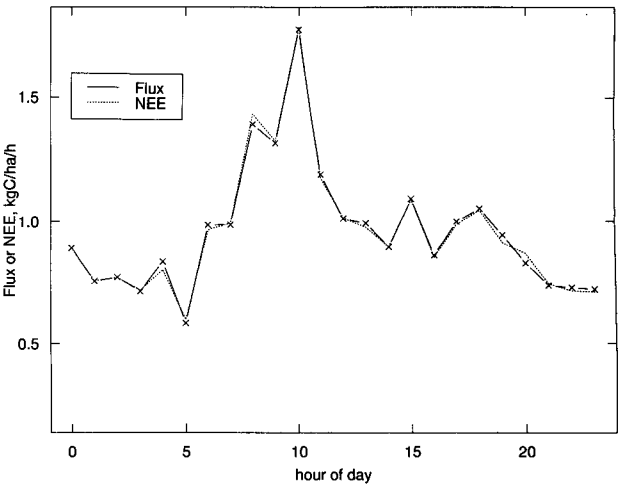

FIG. 12. Hourly median subcanopy (11 m) CO_2 flux and net ecosystem exchange for days 210–250 in 1992.

d. Subcanopy CO_2 flux

Seasonal below-canopy CO_2 flux peaked in midsummer. This is in distinct contrast to the 11-m heat flux that has its peaks in spring and fall. The carbon dioxide flux was measured at the 11-m level during the summer and fall of 1992. During this period, the net flux was nearly always upward (Fig. 12). The flux reaches a maximum in the morning as mixing through the canopy increases (u_* in the subcanopy space greater than 0.08 m s^{-1} median). Baldocchi and Meyers (1991) reported that the autumn CO_2 flux at 2 m in a Tennessee deciduous forest had a sharp peak in the midmorning, instead of being in phase with the measured σ_w. They attribute this to the fact that the root respiration was suppressed under drought conditions and that CO_2 was coming primarily from layers below the leaf litter, causing a decoupling of the flux from static pressure fluctuations.

The median midday flux of carbon in CO_2 in the month of August was 1.6 kg ha^{-1} h^{-1}, which can be compared with the midday above-canopy flux of −9 kg ha^{-1} h^{-1} during this time (Wofsy et al. 1993). The mean daily subcanopy CO_2 flux for the period from late July to late December (days 210–360) was directly related to soil temperature by the relation

$$F_{CO_2} = -0.4074 + 0.0669T, \quad R^2 = 0.49, \quad (5)$$

where F_{CO_2} (kg ha^{-1} h^{-1}) is the flux of CO_2 carbon and T (°C) is the soil temperature at 2-cm depth. Eddy correlation flux data are available for 130 days during this period, many more than have been available for any previously reported measurement of this type (e.g., Baldocchi and Meyers 1991).

The CO_2 concentration profiles from the subcanopy layer were used to obtain an estimate of soil respiration, assuming there was no significant advection from or to the layer. The CO_2 builds up in the subcanopy layer from 0000 to 0500 (LST) but is quickly evacuated or used in the hours 0600–0900. It increases again from 1300–1600. The rate of buildup is small compared to the flux, so that late afternoon buildup increases net ecosystem exchange (NEE) by less than 2% over what the flux at 11 m alone would indicate. The NEE for the layer below 11 m is defined (Wofsy et al. 1993) as

$$\text{NEE} = F + \frac{d}{dt}\int_0^{11} c(z)dz, \quad (6)$$

where F is the flux at 11 m and the second term is the time rate of change of the integrated concentration profile. For the late July–late December period in 1992 we find that the nocturnal NEE is

$$\text{NEE} = -0.2425 + 0.0583T, \quad R^2 = 0.24. \quad (7)$$

Both of these relationships have very similar slopes to that reported for nighttime NEE by Wofsy et al. (1993) (Fig. 13). This is remarkable because the flux relation given (3) is for midday values, rather than for the night NEE. We conclude that the subcanopy layer contributes little as a sink for CO_2 and that the observed midday subcanopy flux is primarily a measure of the subcanopy respiration rate, which is the sum of the soil respiration and leaf and stem respiration to the 11-m level. Thus, the midday eddy correlation flux in the subcanopy layer represents an alternative measure of the respiration rate.

Chamber estimates of respiration rates (Goulden, unpublished data) for various components of the forest are as follows: for soil, 2–3; for leaf, 0.5–1.5; and for stems, 0.1–0.3 kg ha^{-1} h^{-1}. The leaf respiration rates are comparable to the offset between the Wofsy et al. (1993) NEE plot and ours (Fig. 13). However, the chamber measurements of soil respiration are much higher than either of the eddy-correlation-based estimates. Disparities between chamber-based respiration

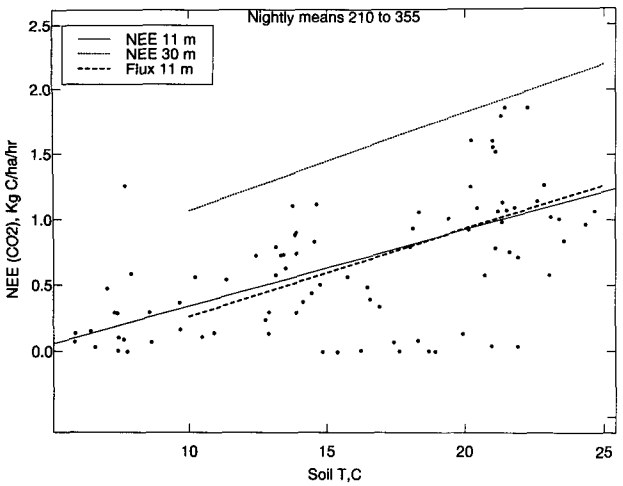

FIG. 13. Net ecosystem exchange of CO_2 (kg °C ha^{-1} h^{-1}) against soil temperature at 5-cm depth for days 210–355 in 1992. The relationships for flux at 11 m and for NEE at 30 m (Wofsy et al. 1993) are also shown.

estimates and eddy-correlation estimates are common. Further analysis of the sources of error in the methods is in preparation by Goulden.

5. Conclusions

This paper has presented an overview of the seasonal changes observed in the turbulent and radiative fluxes at Harvard Forest. We have made the first steps toward using remote sensing for estimates of flux by linking the seasonal changes in surface fluxes to those in in situ radiation measurements. Solar albedo is a reliable indicator of the presence of leaves and of fresh snowfall. We have shown that the aging of canopy during the growing season is detectable in radiative quantities. We suggest that the canopy is not physiologically static during the growing season. On the shorter timescales of days and weeks, factors other than canopy physiology, such as soil moisture, weather, cloudiness, boundary layer growth, saturation deficit, etc., also have variations, and these factors almost certainly influence the surface turbulent exchange properties.

Subcanopy exchange is acutely tuned to the presence or absence of leaves in the overstory. In this deciduous forest, large changes in the subcanopy environment accompanied the leaf emergence and leaf fall periods, including a shift in the energy partition and in the mean states of humidity and temperature. The subcanopy CO_2 flux peaked in the midsummer, while the subcanopy sensible heat flux was a maximum in spring and fall just prior and subsequent to leaf out and leaf drop, respectively. Subcanopy evapotranspiration was 10%–11% of that above the canopy during the growing season. Daytime subcanopy CO_2 flux obtained using the eddy-correlation method is comparable to the nighttime respiration rate determined above the canopy. Work is in progress to use the measurements at Harvard Forest to drive a surface exchange model such as SiB (Sellers et al. 1986) and to use satellite data to explore the representativity of the Harvard Forest site.

Much work remains to be done to relate remote sensing variables to surface exchange features. This is an essential element in the process of scaling up surface observations such as those at Harvard Forest to the regional, or larger, scales. The long-term nature of the turbulent exchange measurements at Harvard Forest affords us the opportunity to sort out the effects of factors on a wide variety of scales from the turbulent to the synoptic, seasonal, and interannual.

Acknowledgments. One hundred percent ($94,000 per year) of this research was funded by the US Department of Energy's (DOE) National Institute for Global Environmental Change (NIGEC) through the NIGEC Northeast Regional Center at Harvard University. (DOE Cooperative Agreement DE-FC03-90ER61010.) Financial support does not constitute an endorsement by DOE of the views expressed in this article/report. The work at SUNY is supported by subcontract 901214 from Harvard University, under the Northeast Regional Center of the National Institute for Global Environmental Change, to the Research Foundation of the State University of New York.

Some data used in this publication were obtained by scientists of the Hubbard Brook Ecosystem Study and accessed by the present authors via the World Wide Web. This publication has not been reviewed by those scientists. The Hubbard Brook Experimental Forest is operated and maintained by the Northeastern Forest Experiment Station, U.S. Department of Agriculture, Radnor, Pennsylvania.

The excellent technical assistance of Mr. John W. Sicker is acknowledged.

REFERENCES

Baldocchi, D. D., and T. P. Meyers, 1991: Trace gas exchange above the floor of a deciduous forest. Part 1. Evaporation and CO_2 flux. *J. Geophys. Res.*, **96,** 7271–7285.

Barradas, V. L., and J. Adem, 1992: Albedo model for a tropical dry deciduous forest in western Mexico. *Int. J. Biometeor.*, **36,** 113–117.

Betts, A. K., 1994: Relation between equilibrium evaporation and the saturation pressure budget. *Bound.-Layer Meteor.*, **71,** 235–245.

Bormann, F. H., and G. E. Likens, 1979: *Pattern and Process in a Forested Ecosystem.* Springer-Verlag, 253 pp.

Culf, A. D., 1994: Equilibrium evaporation beneath a growing convective boundary layer. *Bound.-Layer Meteor.*, **70,** 37–49.

DeBruin, H. A. R., 1983: A model for the Priestley–Taylor parameter α. *J. Climate Appl. Meteor.*, **22,** 572–578.

Dorman, J. L., and P. J. Sellers, 1989: A global climatology of albedo, roughness length and stomatal resistance for atmospheric general circulation models as represented by the Simple Biosphere Model (SiB). *J. Appl. Meteor.*, **28,** 833–855.

Esau, K., 1965: *Plant Anatomy.* John Wiley and Sons, 767 pp.

Fitzjarrald, D. R., and K. E. Moore, 1994: Growing season boundary layer climate and surface exchanges in a subarctic lichen woodland. *J. Geophys. Res.*, **99,** 1899–1917.

——, and ——, 1995: Physical mechanisms of heat and mass exchange between forests and the atmosphere. *Forest Canopies,* M. D. Lowman and N. M. Nadkarni, Eds., Academic Press, 624 pp.

Foster, D., 1992: Land-use history (1730–1990) and vegetation dynamics in central New England, USA. *J. Ecol.,* **80,** 753–772.

Gallo, K., 1992: Experimental calibrated global vegetation index. NOAA National Environmental Satellite, Data, and Information Service. Boulder, CO, 34 pp.

Gates, D., 1980: *Biophysical Ecology.* Springer-Verlag, 611 pp.

Hunt, E. R., and B. N. Rock, 1989: Detection of changes in leaf water content using near- and middle-infrared reflectances. *Remote Sens. Environ.,* **30,** 43–54.

Kuhn, M. H., 1989: The role of land ice and snow in climate. *Understanding Climate Change,* A. Berger, R. E. Dickinson, and J. W. Kidson, Eds., International Union of Geodesy and Geophysics, *Geophys. Monogr.* No. 52, Amer. Geophys. Union, 187 pp.

Latimer, J. R., 1978: Radiation measurement. Int. Field Year for the Great Lakes. Tech. Manual Ser. 2, 37 pp.

Laubach, J., M. Raschendorfer, H. Kreilein, and G. Gravenhorst, 1994: Determination of heat and water vapour fluxes above a spruce forest by eddy correlation. *Agric. For. Meteor.,* **71,** 373–401.

Lu, C.-H., and D. R. Fitzjarrald, 1994: Seasonal and diurnal variations of coherent structures over a deciduous forest. *Bound.-Layer Meteor.,* **69,** 43–69.

Luvall, J. C., and H. R. Holbo, 1991: Thermal remote sensing methods in landscape ecology. *Quantitative Methods in Landscape Ecology,* M. G. Turner and R. H. Gardner, Eds., Springer-Verlag, 127–215.

McCaughey, J. H., 1987: The albedo of a mature mixed forest and a clear-cut site at Petawawa, Ontario. *Agric. For. Meteor.,* **40,** 251–263.

McMillen, R. T., 1986: A BASIC program for eddy correlation in non-simple terrain. NOAA Tech. Memo. ERL ARL-147.

Monteith, J. L., 1965: Evaporation and environment. *The State and Movement of Water in Living Organisms,* G. E. Fogg, Ed., Academic Press, 1–47.

Moore, C. J., 1986: Frequency response corrections for eddy correlation systems. *Bound.-Layer Meteor.,* **37,** 17–35.

Munger, J. W., S. C. Wofsy, P. S. Bakwin, S.-M. Fan, M. L. Goulden, B. C. Daube, A. H. Goldstein, K. E. Moore, and D. R. Fitzjarrald, 1995: Atmospheric deposition of nitrogen oxides and ozone and a temperature deciduous forest and a sub-arctic woodland. 1. Measurements and mechanisms. *J. Geophys. Res.,* in press.

Nemani, R. R., and S. W. Running, 1989: Estimation of regional surface resistance to evapotranspiration from NDVI and thermal-IR AVHRR data. *J. Appl. Meteor.,* **28,** 276–284.

Oke, T. R., 1987: *Boundary Layer Climates.* Methuen, 435 pp.

Panofsky, H. A., and J. A. Dutton, 1984: *Atmospheric Turbulence.* John Wiley and Sons, 397 pp.

Peixoto, J. P., and A. H. Oort, 1992: *Physics of Climate.* American Institute of Physics, 520 pp.

Robinson, D. A., and G. Kukla, 1984: Albedo of a dissipating snow cover. *J. Climate Appl. Meteor.,* **23,** 1626–1634.

Sakai, R. K., 1995: Leaf area index influence on turbulent exchange in a deciduous forest. M.S. thesis, Department of Atmospheric Sciences, State University of New York at Albany, 128 pp.

Sellers, P. J., Y. Mintz, Y. C. Sud, and A. Dalcher, 1986: A simple biosphere model (SiB) for use within general circulation models. *J. Atmos. Sci.,* **43,** 505–531.

——, F. G. Hall, G. Asrar, D. E. Strebel, and R. W. Murphy, 1992: An overview of the First International Satellite Land Surface Climatology Project (ISLCSP) Field Experiment (FIFE). *J. Geophys. Res.,* **97**(D17), 18 345–18 371.

——, and Coauthors, 1995: The Boreal Ecosystem–Atmosphere Study (BOREAS): An overview and early results from the 1994 field year. *Bull. Amer. Meteor. Soc.,* **76,** 1549–1577.

Shaw, R. H., G. den Hartog, and H. H. Neumann, 1988: Influence of foliar density and thermal stability on profiles of Reynolds stress and turbulence intensity in a deciduous forest. *Bound.-Layer Meteor.,* **45,** 391–409.

Verma, S. B., P. J. Sellers, C. L. Walthall, F. G. Hall, J. Kim, and S. J. Goetz, 1993: Photosynthesis and stomatal conductance related to reflectance on the canopy scale. *Remote Sens. Environ.,* **44,** 103–116.

Wofsy, S. C., M. L. Goulden, J. W. Munger, S.-M. Fan, P. S. Bakwin, B. C. Daube, S. L. Bassow, and F. A. Bazzaz, 1993: Net exchange of CO_2 in midlatitude forests. *Science,* **260,** 1314–1317.